

## Towards (scalable) quantum simulations in ion traps

T. SCHAETZ\*, A. FRIEDENAUER, H. SCHMITZ,  
L. PETERSEN and S. KAHRA

Max Planck Institut für Quantenoptik, Hans Kopfermann Strasse 1,  
85748 Garching, Germany

(Received 14 March 2007; in final form 14 August 2007)

Experiments directed towards the development of an analogue quantum simulator based on trapped atomic magnesium ions are described. We report on the required initialization including ground state cooling of  $^{25}\text{Mg}^+$  ions for the first time—parallel to the group at NIST/Boulder. We discuss basic operations to implement quantum spin Hamiltonians like a one-dimensional quantum Ising model and some challenges to be addressed in reaching for larger scale and higher dimensional devices.

### 1. Introduction

Simulations and the related deeper understanding of the dynamics of some tens of interacting quantum bits (qubits) are already intractable for the most powerful classical computers. For instance, the generic state of 30 spin- $\frac{1}{2}$  particles is defined by  $2^{30}$  numbers and to describe its evolution a matrix of  $2^{30} \times 2^{30}$  has to be exponentiated [1]. Even exponentially increasing classical calculation capabilities cannot help to efficiently simulate only slightly larger quantum systems [2]. Already for 300 particles  $2^{300}$  numbers describe the state, close to the guestimated amount of protons in (one of) our universe(s).

As originally proposed by Feynman [3], a quantum computer could efficiently simulate the dynamics of many-body quantum systems. A very promising candidate might be one based on trapped ions [4]. On the other hand, to realize a universal quantum computer, i.e. capable of running arbitrary algorithms, one will have to have control to the order of  $10^5$  qubits [2]. Even though there appear to be no fundamental limits in scaling the required apparatus, there is still challenging technology to be developed, with a time scale probably measured in decades. Thus, to gain deeper insight into the dynamics of quantum systems, an alternative approach should be taken into consideration.

---

\*Corresponding author. Email: tschaetz@mpq.mpg.de

Instead of translating quantum dynamics into an algorithm and running it on a universal quantum computer, one could choose a system to be controlled and manipulated with its evolution being governed by the same Hamiltonian as the system to be simulated [5]. More importantly, one could call this analogue quantum simulator a quantum computer designed to address a certain set of problems in an even more efficient way than a universal quantum computer.

The Hamiltonians that can be realized with trapped ions, can show a Heisenberg-like interaction [1, 5]. Quantum spin Hamiltonians of this type describe magnetism in many solid-state systems like magnets, high- $T_c$  superconductors, quantum Hall ferromagnets, ferroelectrics etc., and their simulation would allow one to observe and analyse quantum phase transitions [5].

As a basic example, we describe the quantum Ising model, involving already all the important ingredients for the quantum spin Hamiltonians listed above and we discuss how the simulation could be implemented in an ion trap. The quantum Ising Hamiltonian ( $H_{\text{Ising}} = J \sum_{m=n+1} \sigma_m^z \sigma_n^z + B_x \sum_m \sigma_m^x$ ) consists of two contributions. The first part represents the interaction between the spins of nearest neighbours in the 1D-spin chain, where the amplitude of  $J$  describes the interaction strength while its positive (negative) sign stands for an anti-ferromagnetic (ferromagnetic) interaction. The latter part can be understood as the interaction of a magnetic field  $B_x$  with each spin independently.

## 2. Experimental setup and procedure

In the following we describe how we plan to realize the simulation of a ‘baby’ quantum phase transition with two to three qubits [6] by applying operations closely related to those implemented on qubit-ions in quantum information processing [7] and summarize the current status in our laboratory.

After photoionizing atoms in a thermal beam of Mg atoms [8] in the loading zone of our linear radio-frequency trap, similar to that described in [9, 10], we confine two to three  $^{25}\text{Mg}^+$  ions along the trap axis and transfer them into our experimental zone via switching appropriate voltages on the segmented DC electrodes depicted in figure 1(c).

The required simulation basis can be composed of two  $^2S_{1/2}$  electronic ground state levels of the  $^{25}\text{Mg}^+$  ion, here the states  $|F=3; m_f=3\rangle \equiv |\downarrow\rangle$  and  $|F=2, m_f=2\rangle \equiv |\uparrow\rangle$ , separated by the hyperfine splitting  $\omega_o \simeq 2\pi \times 1.8$  GHz, as depicted in figure 1(a). In addition, we show the harmonic oscillator levels  $|n\rangle$  related to the axial harmonic confinement.

We accomplish the coupling of the two internal states  $|\downarrow\rangle$ ,  $|\uparrow\rangle$  and the motional states  $|n\rangle$  via off-resonant two-photon stimulated Raman transitions [7] requiring two laser beams ( $\lambda \approx 280$  nm), depicted as beams (i) in figure 1(a). The wave vector difference  $\Delta\mathbf{k} = \mathbf{k}_2 - \mathbf{k}_1$  is aligned along the trap axis  $z$  ( $|\Delta k| = 2^{1/2} \times 2\pi/\lambda = 2\pi/\lambda_{\text{eff}}$ ). The frequency difference  $\omega_2 - \omega_1$  being equal to  $\omega_o \pm 2\pi \times m\nu_z$  can be changed by integer multiples  $m$  of the axial trapping frequency  $\nu_z$  to drive the carrier transition ( $m=0$ ), the first- ( $m=1$ ) or even higher sideband transitions, respectively. To implement the effective magnetic field  $B_x$ , we drive the carrier

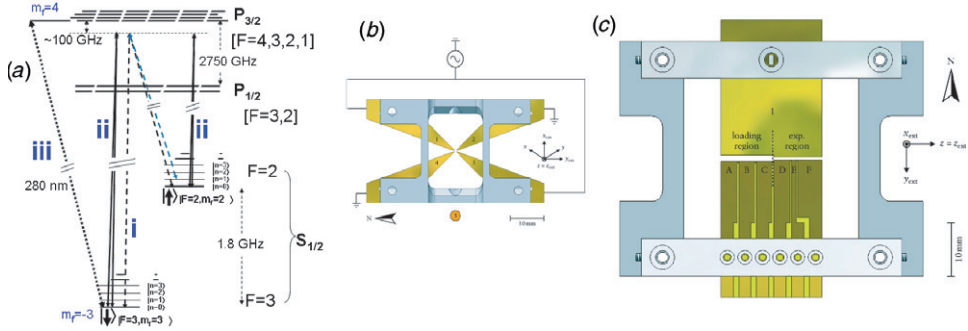


Figure 1. (a) Schematic of relevant energy levels (not to scale) of one  $^{25}\text{Mg}^+$  ion. Shown are the ground-state hyperfine levels supplying the two internal states ( $|\downarrow\rangle$  and  $|\uparrow\rangle$ ) and the equidistant harmonic oscillator levels  $|n\rangle$ , related to the harmonic axial (or radial) confinement in a linear ion trap. We subsumed the levels of the  $P_{1/2}$  and  $P_{3/2}$  states. Typically, the energy splitting of the motional levels and the Zeeman shift induced by an external magnetic field are of the same order of magnitude within 1–10 MHz, therefore much smaller than the hyperfine splitting of 1.8 GHz, the fine structure splitting of 2750 GHz and the optical transition frequency of the order of  $10^{15}$  Hz. We depict the resonant transition state sensitive detection named (iii), the relevant types of off-resonant ( $\approx 100$  GHz) two-photon stimulated Raman transitions providing the AC-Stark shift and the state dependent optical dipole force (ii) and the coupling between the qubit states (i), further described in the text. (b) View along the trap axis and (c) top view on the segmented linear ion trap providing a loading and an experimental zone. With its RF-driving frequency of  $2\pi \times 60$  MHz, and minimal distance between the RF electrodes of  $800 \mu\text{m}$  it allows for secular frequencies up to  $2\pi \times 6$  MHz and simulation experiments for up to 10 qubits. (The colour version of this figure is included in the online version of the journal.)

transition leading to a rotation of the state vector on the Bloch sphere equivalent to the rotation of a spin around the axis defined by an applied magnetic field.

Regarding the realization of a spin–spin interaction it should be mentioned that a typical spacing of the ions  $\geq 3 \mu\text{m}$  is large enough to make the direct spin–spin interaction negligible. The simulated effective spin–spin interaction is mediated via an internal state-dependent AC-Stark shift. We induce it by beams (ii) in figure 1(a), giving rise to a state-dependent optical dipole force that translates via a canonical transformation to the envisioned effective spin–spin interaction [5].

The parameters of the Hamiltonian can be manipulated independently. Changing the intensity of the laser beams providing the effective magnetic field  $B_x$  alters the field amplitude, changing the intensity of the beams providing the optical dipole force alters the amplitude of the interaction strength  $|J|$ . The sign of  $J$  can be controlled via the relative angle between the optical dipole force and  $z$  axis defined by the ion string, i.e. the relative direction of the laser beams. The range of interaction can be tuned by the radial trapping potential.

At the start of each experiment, the ions are laser cooled close to the ground state of the axial (external) motion and optically pumped into the electronic (internal) state  $|\downarrow\rangle$  [11]. At the end, we have to read out the internal state populations. We apply an additional resonant laser beam (iii) in figure 1(a), tuned to a cycling transition [7], coupling only state  $|\downarrow\rangle$  resonantly to the  $P_{3/2}$  level and scattering

photons at rates of 10 MHz. This allows one to distinguish the ‘bright’  $|\downarrow\rangle$  from the ‘dark’  $|\uparrow\rangle$  states with high accuracy, even at a low detection efficiency, mainly due to the restricted solid angle and limited detection efficiency.

The implementation of the most basic protocol for the two and three qubit case, respectively, could be done in the following way: (1) initialize the two (three) qubits in the motional ground state via sideband cooling and in the internal state  $|\downarrow\downarrow\rangle$  ( $|\downarrow\downarrow\downarrow\rangle$ ) via optical pumping. (2) Switch on adiabatically an effective magnetic field  $B_x$  simulated by Rabi-flopping on transition (ii). (3) Switch on adiabatically the effective spin–spin interaction  $J$  simulated by the state-dependent optical dipole force along (perpendicular to) the trap axis via beams (i). (4) Read out the average state of the qubits via transition (iii). In the case of an anti-ferromagnetic transition the qubit ensemble will end up in one of two possible configurations, either  $|\downarrow\uparrow\downarrow\rangle$  or  $|\uparrow\downarrow\uparrow\rangle$ . Even more interesting might be the case of vanishing bias fields where both of these outcomes are ground states of the system. The system should end up in a superposition state of the two possibilities, for example  $|\downarrow\uparrow\downarrow\rangle + |\uparrow\downarrow\uparrow\rangle$  representing a maximally entangled state of all participant qubits.

State of the art techniques allow us to cool the axial motion close to the ground state, as depicted in figure 3(b), with our best results indicating  $\bar{n} \approx 0.05$  and in the future possibly even below [10, 11] and to optically pump into the down state with 99% or even higher fidelity [10, 11].

Since the state of the art fidelities for the carrier and sideband transitions as well as the state sensitive detection exceed 99% [10, 11], the initialization and measurement of the system can be provided with high accuracy.

The main task to benefit from these envisioned operational fidelities will be to minimize disturbances during the whole simulation period, for example fluctuations of the magnetic field and the laser intensities via active compensation. It might ease the requirements that the duration of the experiment will be short ( $\approx 2$  ms) compared to the inverse of the thermal heating rate for motional quanta measured in the trap ( $\leq 0.05$  quanta  $\text{ms}^{-1}$ ).

To perform the envisioned study of feasibility, all earth alkaline ions and even more might be used. However, lighter ions provide advantages for a future scaling discussed in section 3, mostly to their tighter confinement. Since the radial trapping potential is inversely proportional to the mass of the ions, lighter ions can be trapped in a stable way in shallower traps, as the surface traps [11] or any other miniaturized setup necessary for scaling<sup>†</sup>.

---

<sup>†</sup>Be<sup>+</sup>, even lighter than Mg<sup>+</sup> suffers other disadvantages. For example, it cannot be photo-ionized in an easy way like Mg [8]. State-of-the-art electron impact ionization is potentially responsible for charging up and becoming an increasing problem for the envisioned closer lying surfaces. In addition it requires of the order of three expensive and high maintenance dye-laser systems. Our choice of <sup>25</sup>Mg<sup>+</sup> as qubit ions required the development of an affordable solid state based laser source for light of 280 nm at a beam power exceeding 300 mW. After developing and setting up three of these systems [13], we were able to drive coherent oscillations in Mg ions for the first time, as depicted in figure 2. In addition we cooled one <sup>25</sup>Mg<sup>+</sup> to its motional ground state for the first time as shown in figure 3.

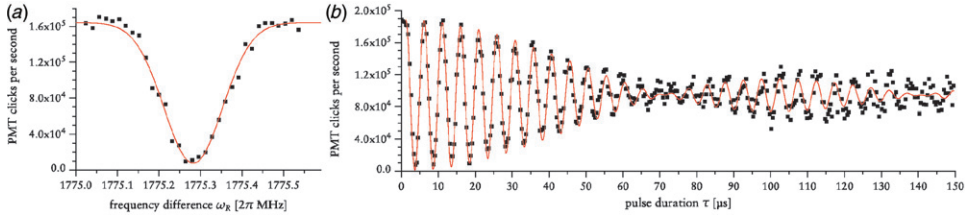


Figure 2. First experiments showing the averaged count rate measured by a photo multiplier (PMT) of one  $^{25}\text{Mg}^+$  ion with dependence on the detuning or duration of the copropagating Raman pulses preceding a final resonant detection pulse. Ideally, maximal count rate represents the ion in state  $|\downarrow\rangle$  while zero count rate corresponds to the ion in the state  $|\uparrow\rangle$ . The solid lines are fits to the experimental data. (a) Spectrum recorded with dependence on the frequency difference between the two Raman beams for a constant duration of the probe pulse. The minimal count rate occurs at resonant conditions where the population is almost completely transferred from the  $|\downarrow\rangle$  into the  $|\uparrow\rangle$  state. (b) Coherent oscillations recorded with dependence on the variation of the pulse duration for constant and close to zero detuning from the resonant transition. For a discussion of the reduction of the contrast and decoherence effects damping the oscillations we refer to the text. (The colour version of this figure is included in the online version of the journal.)

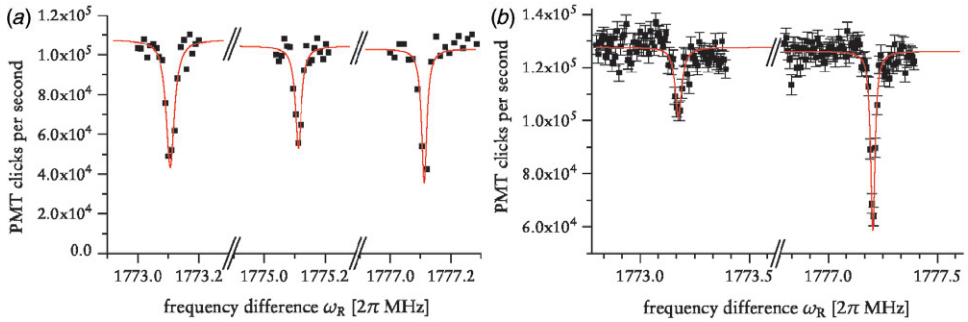


Figure 3. First experiments on initializing one  $^{25}\text{Mg}^+$  ion after (a) Doppler cooling and (b) additional resolved sideband cooling and optical pumping. The spectra are recorded with dependence on the frequency difference between the two orthogonal Raman beams at a constant duration of the probe pulse. The minimal count rates occur at resonant conditions where the population is almost completely transferred from the  $|\downarrow\rangle|n\rangle$  into the  $|\uparrow\rangle|n-1\rangle$  (red-sideband),  $|\uparrow\rangle|n\rangle$  (carrier) or  $|\uparrow\rangle|n+1\rangle$  blue-sideband state. (a) After simple Doppler cooling, a thermal distribution of the motional state with an average motional state occupation of  $\bar{n} \approx 10$  is reached providing approximately the same contrast for the two sideband transitions. (b) Additional resolved sideband cooling provides, in the depicted first shot experiments, more than 60% of the population in the motional ground state with  $\bar{n} \leq 0.5$ . Since the red-sideband transition cannot be driven any more for ions in the motional ground state, its reduced contrast compared to the blue sideband transition allows for determining  $\bar{n}$ . Our best results provide us with  $\bar{n} \approx 0.05$ . (The colour version of this figure is included in the online version of the journal.)

Increasing the system towards 8 qubits might be feasible by this proposal with state-of-the-art techniques [14], further scaling might benefit from the technical progress driven by the attempts of the quantum information community [4] and described below.

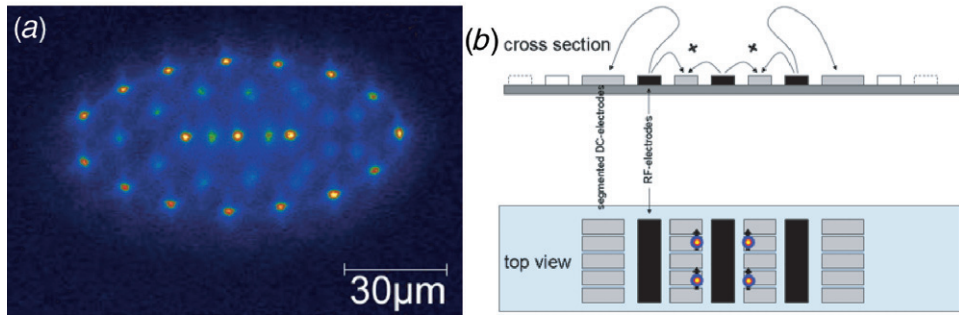


Figure 4. Possibilities to increase the amount of simulation ions and dimensions for an analogue quantum simulator. (a) Image of a two- to three-dimensional Coulomb crystal of approximately  $40 \text{ }^{25}\text{Mg}^+$  ions taken by our CCD camera in the experimental zone of our trap. Difficulties on scaling this system in one single linear ion trap and/or to apply quantum simulations within are discussed in the text. (b) Schematic view of an ion trap with the RF (black bars) and segmented DC electrodes projected on a surface. We plan to position segmented linear ion traps at a distance that allows for stiff single ion confinement and a Coulomb interaction between ions being similar in two dimensions. If we were able to master the technical challenges we could construct a two-dimensional trap array and test the scalability for two-dimensional quantum simulations. (The colour version of this figure is included in the online version of the journal.)

### 3. Scalability of the quantum simulation approach

Besides the task of providing the feasibility test for quantum simulations in ion traps involving several simulation ions only, there remains the fundamentally and technically important challenge to develop methods that allow for scaling the simulator to a large number of qubits and/or more dimensional systems, as proposed in this paper.

In state-of-the-art linear Paul ion traps we can store one-, two- and three-dimensional Coulomb crystals. As an example see figure 4(a). Even though there might be fruitful applications in the field of small-scale quantum simulations, several drawbacks seem to hinder further scaling. Ions confined in a linear Paul trap can only be brought to rest if they are aligned along the trap axis, therefore allowing scalable conditions in a first step only for one-dimensional structures<sup>‡</sup>.

But even for a given one-dimensional structure, the distances of the ions along the chain are not homogeneous. The ions that are not placed in the centre of the chain will experience a reduced Coulomb repulsion leading to an increased inter-ion distance towards the ends of the chain and therewith a reduced interaction to be simulated. In addition, for each ion added, three new motional modes have to be taken into account in the motional spectrum causing all possible combinations of

<sup>‡</sup>Displacement from the trap axis, for example by the Coulomb interaction in a two- or three-dimensional crystal, leads to so-called micro-motion. The simple time-averaged pseudo potential of the trap gets an additional contribution due to the fact, that the ion is closer to one RF electrode than to the others driving an oscillation at the RF frequency of the trap.

sum and difference frequencies to appear. To address the individual mode of interest, for example for cooling the motional modes close to their ground states, one has to increase the spectral resolution for each ion. Starting too far from the ideal conditions, for example due to insufficient cooling caused by missing spectral resolution, we increase the intrinsic errors of the simulation [5].

To circumvent these difficulties in the approach towards a universal quantum computer, Dave Wineland suggested a net of interconnected linear ion traps functioning as memory or processor traps that provides the possibility to shuttle qubits individually in between and should allow for scaling up to a large amount of qubits [15]. It has to be mentioned that this multiplex approach is not applicable to analogue quantum simulations, where the whole ensemble is supposed to evolve adiabatically and uniformly. Splitting the system into several sub-systems would provide the basis for the simulation of a different Hamiltonian—most likely not the one of fundamental interest.

Significant progress towards scalability of the universal quantum computer and the analogue quantum simulator was made by introducing micro-fabrication techniques combined with new trapping geometries [12]. All electrodes required reside on one single surface with the ions being trapped above it.

For the multiplex ion-trap architecture this might allow one to interconnect linear ion traps on a two-dimensional surface to a lattice of one-dimensional traps. We hope to take advantage of these techniques but push towards a different objective, a real two-dimensional trap. We want to place linear ion traps close enough beside each other to provide stiff and controllable confinement of each ion individually, but to allow for sufficient Coulomb coupling not only between ions confined in the same linear trap, but also between ions trapped in neighbouring traps [16]. A first step towards this direction is depicted in figure 4(b). There are several advantages and challenges to be mentioned.

Trapping the simulator ions in a two-dimensional grid would place them at constant nearest neighbour distance, thus, simplifying equal phase of laser beams and interaction strength, respectively. Due to the disentanglement between the strength of confinement and the inter-ion distance, we could choose a strong enough individual trapping for effective cooling close to the motional ground state and get a weak but a possibly strong enough coupling between the ions mediated via Coulomb interaction [5]. Each lattice site could be loaded by shuttling ions along the segmented DC electrodes and addressed individually for simulation and/or detection perpendicular to the plane of the lattice. To realize the global and uniform interaction we would illuminate the ions parallel to the plane of the lattice and perform a strongly astigmatic laser beam by a final cylindrical lens to minimize the constraints on the total laser power actually available [13].

The drawbacks or technical challenges related to this proposal are manifold, mostly related to the proximity to the trap surface, but individually addressable, too.

To realize a distance between simulation ions of the order of  $30\ \mu\text{m}$  and below, the ions will have to be trapped by electrode structures of comparable size leading to trap minima lying comparably close above the surface. On the one hand, we will have to face increased motional heating rates [7], while the coupling interaction will be reduced and therefore the duration for an adiabatic evolution of the system will

be increased [5] making the simulation more vulnerable to decohering effects. On the other hand, recent results concerning reduced heating rates out of the groups in Boulder [12] and Michigan seem to be promising. Further cooling of the apparatus might not only reduce the residual heating rates but also decrease the residual-gas pressure and therefore increase the lifetime of the ions lying now at an improvable 24 h per ion but starting to become a problem with increasing amounts of simulating ions. The proximity to surfaces will also increase the constraints on preventing stray light. In addition, we will have to contact the segmented DC electrodes being isolated from access by surrounding electrodes requiring an additional staking of wires beneath the surface in a multi-layer structure.

As a first step we plan to realize a surface trap allowing for two  $\times$  two qubit-ions with comparable Coulomb-coupling between nearest neighbours in two dimensions. Even though classical computers might be outperformed for systems involving more than 40 qubits, already one has to be able to address simulation problems and provide answers leading towards a deeper understanding of complex quantum behaviour, for example of spin-frustration in two-dimensional spin-lattices.

Leading theoreticians concerned with the problems of solid state physics see this in reach for systems of  $10 \times 10$  [17] or  $20 \times 20$  [18], respectively.

The possibility to control the parameters of the system and to address each single lattice site turn it into a versatile system offering tools for analysis overcoming by far the possibilities in experiments on solid state systems [5]. With individual addressing, we could start with a state representing a particular spin excitation. We could also analyse non-equilibrium dynamics by switching the interactions non-adiabatically.

The advantages of an analogue quantum simulator compared to an universal quantum computer that would simulate the interaction by executing discrete steps composed out of an universal set of gates is perhaps apparent. In searching for robust effects, like quantum phase transitions, there would be no need for fault tolerant gate operations. Also, the read-out of the simulation requires only a measurement of the global fluorescence of all qubit-ions.

## Acknowledgements

The work described in this paper was supported by MPG, MPQ and DFG by the Emmy Noether program. We thank Didi Leibfried for his invaluable input and D. Porras and I. Cirac for most interesting comments.

## References

- [1] E. Jané, G. Vidal, W. Duer, *et al.*, quant-ph/0207011 (2002).
- [2] M.A. Nielsen and I.L. Chuang, *Quantum Computation and Quantum Information*, 1st ed. (Cambridge University Press, Cambridge, 2000).
- [3] R.P. Feynman, F.L. Vernon, R.W. Hellwarth, *J. Appl. Phys.* **28** 49 (1957).
- [4] See, for instance, [http://qist.lanl.gov/qcomp\\_map.shtml](http://qist.lanl.gov/qcomp_map.shtml)
- [5] D. Porras and J.I. Cirac, *Phys. Rev. Lett.* **92** 207901 (2004).
- [6] T. Schaetz, D. Leibfried, J. Chiaverini, *et al.*, *Appl. Phys. B* **79** 979 (2004).

- [7] D.J. Wineland, C. Monroe, W.M. Itano, J. Res. Natl. Inst. Stand. Technol. **103** 259 (1998).
- [8] N. Kjørgaard, L. Hornekaer, A.M. Thommesen, *et al.*, Appl. Phys. B **71** 207 (2000).
- [9] M.A. Rowe, A. Ben-Kish, B. DeMarco, *et al.*, Quantum Inf. Comput. **2** 257 (2002).
- [10] F. Schmidt-Kaler, H. Häffner, H. Gulde, *et al.*, Appl. Phys. B **77** 789 (2003).
- [11] B. King, C.S. Wood, C.J. Myatt, *et al.*, Phys. Rev. Lett. **81**, 1525 (1998).
- [12] S. Seidelin, J. Chiaverini, R. Reichle, *et al.*, Phys. Rev. Lett. **96** 253003 (2006).
- [13] A. Friedenauer, F. Markert, H. Schmitz, *et al.*, Appl. Phys. B **84** 371 (2006).
- [14] D. Leibfried, E. Knill, S. Seidelin, *et al.*, Nature **438** 639 (2005); H. Häffner, W. Haenschel, C.F. Roos, *et al.*, Nature **438** 643 (2005).
- [15] D. Kielpinski, C. Monroe, D.J. Wineland, Nature **417** 709 (2002).
- [16] J.I. Cirac and P. Zoller, Nature **404** 579 (2000).
- [17] D. Feder, private communication (2007).
- [18] J.I. Cirac, private communication (2006).